Differences in the densities of charged defect states and kinetics of Staebler–Wronski effect in undoped (nonintrinsic) hydrogenated amorphous silicon thin films

Mehmet Güneş and Christopher R. Wronski

Citation: Journal of Applied Physics **81**, 3526 (1997); doi: 10.1063/1.365000
View online: http://dx.doi.org/10.1063/1.365000
View Table of Contents: http://scitation.aip.org/content/aip/journal/jap/81/8?ver=pdfcov
Published by the AIP Publishing

Differences in the densities of charged defect states and kinetics of Staebler–Wronski effect in undoped (nonintrinsic) hydrogenated amorphous silicon thin films

Mehmet Güneş[a)]
Department of Physics, Faculty of Science, İzmir Institute of Technology, Gaziosmanpaşa Bulv. No: 16, Çankaya, İzmir, 35210 Turkey

Christopher R. Wronski
Electronic Materials Processing and Research Laboratory, The Pennsylvania State University, University Park, Pennsylvania 16802

(Received 6 December 1996; accepted for publication 6 January 1997)

A variety of undoped (nonintrinsic) hydrogenated amorphous silicon (a-Si:H) thin films was studied in greater detail using steady-state photoconductivity, σ_{ph}, subband-gap absorption, $\alpha(h\nu)$, steady-state photocarrier grating (SSPG), and electron-spin-resonance (ESR) techniques both in the annealed and stabilized light soaked states. The experimental results were self-consistently modeled using a detailed numerical analysis. It was found that large differences in the optoelectronic properties of device quality a-Si:H thin films can only be explained using a gap state distribution which consists of positively charged D^+ defect states above the Fermi level, the neutral D^0 defect states, and the negatively charged D^- defect states below the Fermi level. There are large differences both in the densities of neutral and charged defect states and R ratios in different a-Si:H films in the annealed state. The densities of both neutral and charged defect states increased, however, R ratios decreased in the stabilized light soaked state. Very good agreement was obtained between the densities of neutral defect states measured by ESR and those derived from the numerical analysis in the stabilized light soaked state. The kinetics of the Staebler–Wronski effect was also investigated. There was no direct correlation between the decrease of steady-state photoconductivity and increase of subband-gap absorption. The self-consistent fits to wide range of experimental results obtained with the three Gaussian distributions of charged defect states imply that this model is much better representation of the bulk defect states in undoped hydrogenated amorphous silicon thin films. © *1997 American Institute of Physics.* [S0021-8979(97)01408-4]

I. INTRODUCTION

The concept of charged defect states[1] in undoped hydrogenated amorphous silicon thin films has recently been a large scientific interest. It was first proposed by Adler that a large amount of charged silicon dangling bonds with negative correlation energy existed in undoped a-Si:H films. However, early light induced electron-spin-resonance (LESR) measurements claimed that the electron and hole absorption lines in undoped a-Si:H were roughly equal.[2] Then, it was concluded that an insignificant fraction of dangling bonds is charged. The initial results of photothermal deflection spectroscopy (PDS) and electron-spin-resonance (ESR) measurements showed one-to-one correlation between density of neutral Si dangling bonds and changes in the subband-gap absorption.[3] Later, this was supported by ''the bond-breaking model'' that primary defects in a-Si:H films are the neutral silicon dangling bonds and their light induced kinetics were characterized mainly by ''the $t^{1/3}$ rule.''[4] Furthermore, ''the impurity model,'' which uses the stretched exponentials to describe the kinetics of light induced defect creation,[5] was also based only on the neutral Si dangling bonds with positive correlation energy rather than charged defect states. However, a number of experimental results indicated that the charged defect states are present in undoped a-Si:H films.[6–11] In 1988, the results of ESR and LESR by Shimizu *et al.* showed that a large fraction of defect states is charged states.[6] Similarly, a more careful study of ESR and LESR experiments using band-gap and below band-gap light was carried out on thick (8 and 15 μm) a-Si:H films.[7] The authors showed that the ratio of electron (narrow) to hole (broad) absorption line increases with below band-gap light. It was concluded that these increases were due to excitations from the higher density of the D^- states lying close to valence-band edge. These states were interpreted as surface states instead of bulk defect states. Furthermore, in 1993 a detailed comparison of absorption data and spin density using ESR and LESR experiments showed that there are systematic deviations from the proportionality between the electron and hole absorption lines when high- and low-intensity light are used both in the annealed and light soaked state of a-Si:H films.[11] These results were explained by the presence of a band of positively charged defects D^+ in the region of 0.4–0.7 eV below the conduction band edge. In addition, different ratios of charged to neutral defect densities [$R = (N_{D^+} + N_{D^-})/N_{D^0}$] for different films were also reported. Recently, we have also reported self-consistent analysis of the experimental results using steady-state photoconductivity and subband-gap absorption on intrinsic a-Si:H films ($E_F \sim 0.90$ eV from the conduction band) both in the annealed and light soaked states.[12,13] We showed that only the distribution of charged defect states can self-consistently ex-

a)Electronic mail: mgunes@likya.iyte.edu.tr

 0021-8979/97/81(8)/3526/11/$10.00

plain the results of steady-state photoconductivity and subband-gap absorption spectra both in the annealed and light soaked states.

In this article, we extended our study to a variety of intrinsic and nonintrinsic (undoped) *a*-Si:H films. Their annealed and light soaked states were characterized experimentally in greater detail using steady-state photoconductivity, subband-gap absorption, steady-state photocarrier grating (SSPG), and ESR techniques. The experimental results of subband-gap absorption and steady-state photoconductivity were analyzed using the subband-gap absorption model (SAM)[14] based on the Simmons–Taylor statistics.[15] The results extracted from the numerical analysis were compared directly with those measured by SSPG and ESR carried out on the same *a*-Si:H films.

II. EXPERIMENTAL DETAILS

Steady-state photoconductivity, subband-gap absorption, and hole diffusion length measurements were carried out on around 1-μm-thick, intrinsic ($E_F \geqslant 0.90$ eV) and nonintrinsic (undoped) ($E_F = 0.68$–0.89 eV) *a*Si:H films deposited on 7059 glass substrate. Optical absorption in the visible region of the spectrum was obtained from transmission T and reflection R measurements and was used to normalize subband-gap photoconductivities. The optical gaps were derived from the Tauc relation.[16] The ESR measurements were carried out on films codeposited onto quartz substrates. The annealed state was obtained by heating the samples at 200 °C for 12 h in N_2 ambient and stabilized light soaked state was obtained by illuminating through both sides of the samples for more than 100 h with 1 W/cm^2 white light from an ELH light source filtered with both an IR reflector and IR absorber. Light soaking temperature was maintained below 30 °C for low-intensity soaking and around 40 °C for high-intensity soaking by air cooling through both sides of samples. For the study of kinetics of light induced degradation, light soakings were carried out using a single step soaking procedure in which the samples were light soaked for a certain period of time, measurements were performed, and then the samples were reannealed. This procedure was continued until degradation approached a steady state. Steady-state photoconductivities were measured in the ohmic regime with generation rates from $G = 10^{15}$ to 10^{20} cm^{-3} s^{-1} using volume absorbed light of $\lambda = 687$ nm. The subband-gap photoconductivities, measured using the dual beam photoconductivity (DBP)[14,17] technique with volume generation rates from $G = 10^{15}$ to 10^{18} cm^{-3} s^{-1}, were also carried out in the ohmic regimes of photocurrents. In addition, minority carrier (hole) diffusion length measurements were performed using SSPG technique in National Renewable Energy Laboratory on the same samples under volume absorbed generation rates of around 10^{20} cm^{-3} s^{-1} both in the annealed and stabilized light soaked states.

III. RESULTS AND ANALYSIS

A. Annealed state

A variety of undoped (nonintrinsic) *a*-Si:H films deposited at different substrate temperatures T_s was studied in great detail. The films have atomic hydrogen contents from 20 to 8 at. %, which results in a shift at the optical absorption edge as seen from Fig. 1, and the Fermi levels of 0.90 to 0.70 eV from the electron mobility edge. Examples of steady-state photoconductivities (in the inset) and subband-gap absorption results of two nonintrinsic *a*-Si:H films deposited at 200 and 280 °C are shown as symbols in Fig. 1. The results on these films are also summarized in Table I and compared with those of an intrinsic *a*-Si:H film. The steady-state photoconductivity σ_{ph} increased with T_s and their dependence on generation rate G exhibited sublinear behavior ($\sigma_{ph} \propto G^{\gamma}$), where γ changes from 0.73 to 0.84. The electron mobility lifetime, $\mu\tau$ products measured at $G = 10^{16}$ cm^{-3} s^{-1} increased from 4.3×10^{-6} to 3.8×10^{-5} cm^{-2}/V, similarly the subband-gap absorption increased as T_s changed from 200 °C to 280 °C. The excellent overlap between the subband-gap absorption spectra and T and R results over a

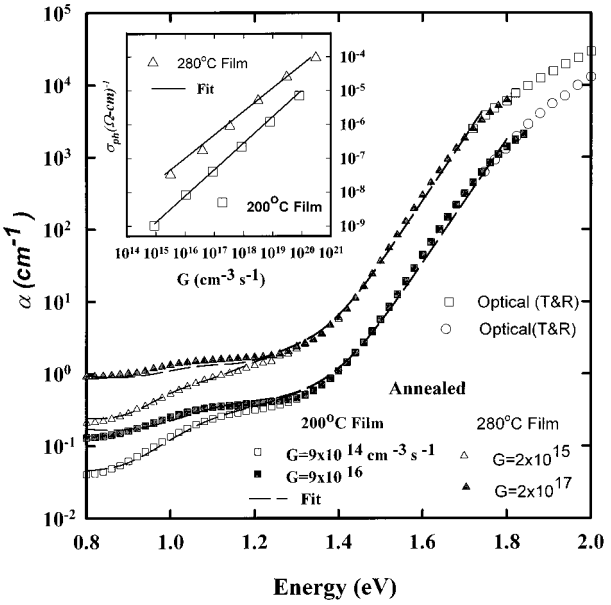

FIG. 1. The experimental results (symbols) of subband-gap absorption spectra of undoped (nonintrinsic) *a*-Si:H thin films deposited at 200 and 280 °C for two different generation rates in the annealed state. The steady-state photoconductivity results (symbols) are shown in the inset. The solid lines are the best fits to the experimental data obtained from the numerical analysis.

TABLE I. A summary of experimental results of nonintrinsic (undoped) *a*-Si:H films and those of an intrinsic *a*-Si:H in the annealed state, where N_{DOS} (cm^{-3}) = α(1.2 eV)$\times 3\times10^{16}$ cm^{-3}.

	Annealed state			
a-Si:H films	280 °C	240 °C	200 °C	Intrinsic
E_{opt} (eV)	1.70	1.74	1.80	1.72
E_F (eV)	0.73	0.84	0.88	0.90
σ_D (S/cm)	1.1×10^{-8}	5.0×10^{-10}	4.0×10^{-11}	2.0×10^{-11}
$\mu\tau$ (cm^2/V) ($G=10^{16}$)	3.86×10^{-5}	5.85×10^{-6}	4.37×10^{-6}	1.9×10^{-6}
γ	0.73	0.84	0.78	0.90
α(1.2) (low G) (cm^{-1})	1.20	0.53	0.28	0.16
E_{ov} (meV)	48	48	49	49
$\Delta\alpha$(1.0 eV) (cm^{-1})	0.90	0.30	0.10	0.06
N_{DOS} (cm^{-3})	3.4×10^{16}	1.5×10^{16}	8.3×10^{15}	5.0×10^{15}

significant energy region eliminates any significant errors in $\alpha(h\nu)$. The subband-gap absorption at 1.2 eV, α(1.2 eV), measured with low generation rate DBP, increased from 0.28 to 1.2 cm^{-1} while the characteristic energy of the valence band tails, E_{ov} remained almost constant at 48 meV. The dependence of $\alpha(h\nu)$ at low energies (from 0.8 to 1.3 eV) on bias light intensity increased with T_s, where $\Delta\alpha$ (at 1.0 eV) [$=\alpha$(1.0 eV) measured at high-intensity DBP-α(1.0 eV) measured at low-intensity DBP] increased from 0.10 to 0.90 as T_s went from 200 to 280 °C. This is an important difference from that observed in intrinsic a-Si:H films (where $E_F \geqslant 0.90$ eV); where $\Delta\alpha$ (at 1.0 eV) was between 0.04 and 0.1.[18]

In general, the $\alpha(h\nu)$ measured with low bias light DBP[14,17] or by the constant photocurrent method (CPM)[19] is related to the density of midgap states, particularly the D^0 states, located below the Fermi level. The advantage of using DBP over CPM is that $\alpha(h\nu)$ measured with high bias light DBP gives information about the density of midgap states both below and above the Fermi level.[14,17] The higher values of $\alpha(h\nu)$ and $\Delta\alpha$ (at 1.0 eV) lead to the presence of a higher density of midgap states, which results in shorter electron lifetimes and lower electron $\mu\tau$ products due to an increase in the density of recombination centers. However, experimental results of electron $\mu\tau$ products of nonintrinsic a-Si:H films increase as subband-gap absorption increases. These increases in the electron $\mu\tau$ products cannot be due to the increases in the free carrier mobilities, because the photomixing experiments carried out on the same set of films indicate that the free carrier mobilities are nearly the same.[20] Therefore, these results discussed above indicate that it is impossible to explain the changes in $\alpha(h\nu)$, $\Delta\alpha$ (at 1.0 eV), and electron $\mu\tau$ products by considering only the neutral Si dangling bonds, the D^0 states, as a main defect in the band gap. There must be more than one type of defect states located in the band gap of a-Si:H. To identify these defect states, detailed numerical analysis of the steady-state photoconductivity and subband-gap absorption spectra as a function of generation rate is necessary.

We have previously reported that two Gaussian distributions of midgap states[4] with positive correlation energy can explain neither the results of nonintrinsic a-Si:H films in the annealed state[21] nor the light soaked state characteristics of intrinsic films.[22] Later, it was shown by us that only the distribution of charged defect states can explain the changes in steady-state photoconductivity and subband-gap absorption spectra self-consistently both in the annealed and light soaked states in intrinsic a-Si:H films.[12,13] In this study, the same distribution of charged defect states as described previously, which is shown in Fig. 2, and the SAM[14] are used to analyze the experimental results of nonintrinsic a-Si:H films.

In the analysis, extended state parameters, free carrier mobilities, free carrier capture cross sections for exponential tail states, and neutral and charged midgap defect states were maintained to be the same as those used in the analysis of intrinsic a-Si:H films.[12,13] For each sample, the experimental values of the optical gap, the Fermi level position, and the characteristic energy of valence band tails E_{ov} were taken into account as key inputs and 21 meV as the characteristic

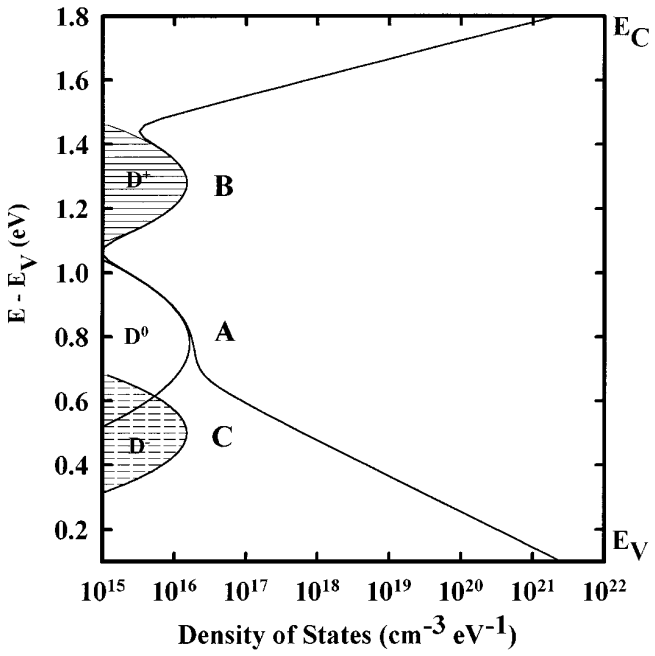

FIG. 2. The energy distribution of gap states including both the neutral and charged defect states used in the self-consistent modeling of σ_{ph} and $\alpha(h\nu)$ measured in undoped a-Si:H thin films.

energy of conduction band tail states was used for all nonintrinsic a-Si: H films.[23] Mobility gap or recombination gap was assumed to be 0.1 eV larger than the optical gap. The half-widths of the Gaussian distributions were similar to those used in intrinsic films and the values were between 0.09 and 0.12 eV. No *a priori* assumptions were made for the densities and exact energy location of neutral and charged defect states. They were derived from the self-consistent fits to steady-state photoconductivity and the subband-gap absorption spectra.

The best fits to the steady-state photoconductivity (in the inset) and subband-gap absorption spectra are also shown in Fig. 1 for a wide range of generation rates for the same nonintrinsic a-Si:H films. (A summary of the derived parameters for the neutral and charged defect states is shown in Table III for nonintrinsic films and an intrinsic a-Si:H film for a comparison.) It is important to note that the density of the neutral defect states is the same in different films but the densities of the charged defect states increase from 9×10^{15} to 6×10^{16} cm^{-3} as the substrate temperature increases from 200 to 280 °C. The derived densities of both the charged and neutral defects are higher than those derived for intrinsic films.[13] The ratio of charged to neutral defect states R is also higher than that in intrinsic films[13] and systematically increases from 2.25 to 15 as T_s increases from 200 to 280 °C. The energy position of neutral defect states is around 0.80 eV from the valence-band edge, which is similar to that obtained from the analysis of intrinsic films. However, both the negatively charged D^- states and positively charged D^+ states lie at higher energies than those in intrinsic films. Nevertheless, the annealed state characteristics of various intrinsic and nonintrinsic a-Si:H films can be explained self-consistently using the same distribution of charged defect

states where the positively charged states are located above the Fermi level and the negatively charged and neutral defect states are located below the Fermi level.

Because of the experimental difficulties, it was impossible to carry out reliable ESR studies for direct comparisons of the D^0 states on these films in the annealed state. However, the derived densities of neutral defect states, the D^0, can be compared with those obtained from the $\alpha(1.2\ \text{eV})\times 3\times 10^{16}$ relation.[12] It can be seen that they are comparable for intrinsic films since the D^0 states dominates subband-gap absorption; but, the $\alpha(1.2\ \text{eV})$ relation generally overestimates the density of the D^0 states for nonintrinsic a-Si:H films in the annealed state because the subband-gap absorption spectrum measured with CPM or low bias light DBP is controlled by both the D^0 as well as the higher density of the charged defect states. Therefore, the subband-gap absorption measured by CPM or low bias light DBP can no longer be related to the densities of the D^0 states using the $\alpha(1.2\ \text{eV})\times 3\times 10^{16}$ relation or by the integration rule[19] in the annealed state of nonintrinsic a-Si:H films.

In addition to the steady-state photoconductivity and subband-gap absorption measurements, the hole diffusion length L_{Dp} was measured on the same nonintrinsic a-Si:H films at the same state using the SSPG technique.[24] In the analyses of σ_{ph} and $\alpha(h\nu)$ only the contributions of free electrons have to be considered even though free and trapped hole concentrations at different generation rates are derived after solving the charge neutrality and recombination rate equations.[15] This allows both free carrier lifetimes τ_n and τ_p to be calculated for a given generation rate. Thus, assuming a free hole mobility (in this case $\mu_p=0.2\ \text{cm}^2/\text{V s}$ for all films), the hole $\mu_p\tau_p$ product can be utilized to calculate the hole diffusion lengths using the relation $L_{Dp}=(2\mu_p\tau_p kT/e)^{0.5}$.[24] (The L_{Dp} values obtained from the best fit parameters of photoconductivities are shown in Table III.) The excellent agreement between the calculated values of L_{Dp} and the experimental results for these films in the annealed state is strong confirmation of the reliability, the charged defect state distribution used, and the gap state parameters derived in the annealed state.

B. Stabilized light soaked state

It is well known that the Staebler–Wronski effect is an intrinsic property of hydrogenated amorphous silicon based materials.[25] According to this effect, when a-Si:H films are exposed to light illumination, dark and photoconductivity decrease,[25] the density of ESR active states increases,[26] and correspondingly the subband-gap absorption increases.[3] The degradation depends upon soaking time, soaking temperature, and intensity of light.[25,27] Therefore, in order to compare various nonintrinsic (undoped) a-Si:H films with different annealed state characteristics, we light soaked them under 1 W/cm^2 uniform white light at low temperatures ($\sim$40 °C) until the stabilized state was reached, where both the subband-gap absorption and steady-state photoconductivity remained unchanged. The experimental results of $\alpha(h\nu)$ and σ_{ph} as a function of generation rate are shown in Figs. 3 and 4 for the films deposited at 200 and 280 °C, respectively, both in the annealed and stabilized light soaked states. The

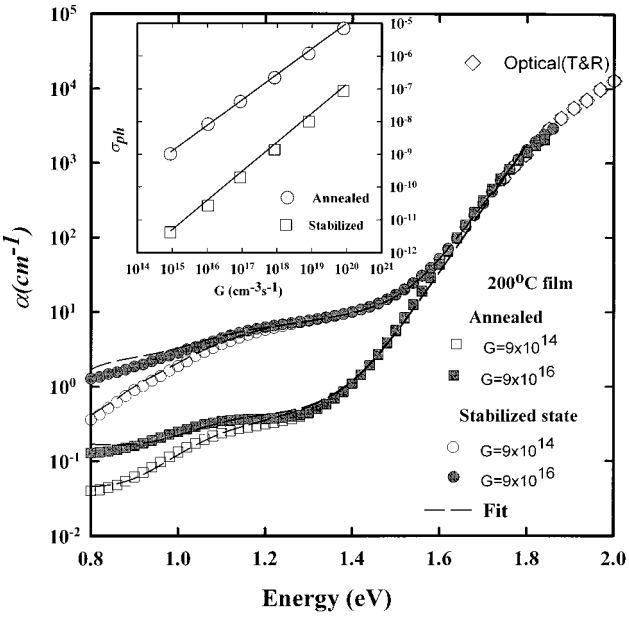

FIG. 3. The experimental results (symbols) of subband-gap absorption spectra of undoped (nonintrisic) a-Si:H thin films deposited at 200 °C for two different generation rates both in the annealed and stabilized light soaked states. The steady-state photoconductivity results (symbols) are shown in the inset. The solid lines are the best fits to the experimental data.

experimental results in the stabilized light soaked state are also summarized in Table II for nonintrinsic films and an intrinsic film for a comparison. According to this table, dark conductivity decreased by a factor of 10 for the 200 °C film, by two orders of magnitude for the 240 °C film, and by almost three orders of magnitude for the 280 °C film. This decrease in dark conductivity is attributed to a shift in the Fermi level position through the midgap.[25,28] The depen-

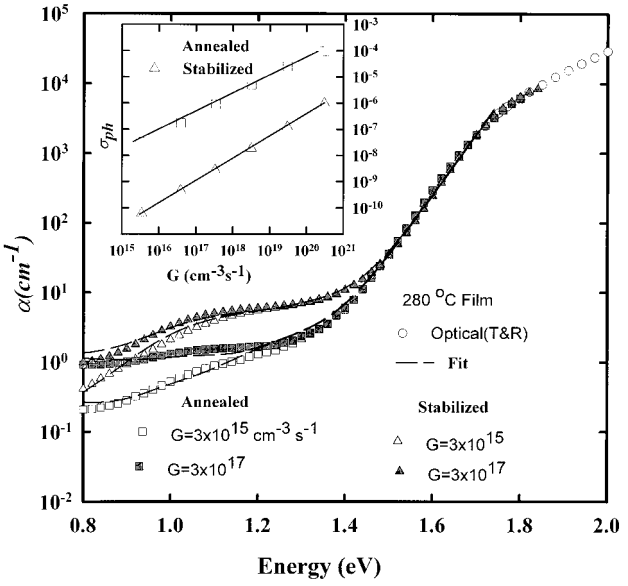

FIG. 4. The experimental results (symbols) of subband-gap absorption spectra of undoped (nonintrincsic) a-Si:H thin films deposited at 280 °C for two different generation rates both in the annealed and stabilized light soaked states. The steady-state photoconductivity results (symbols) are shown in the inset. The solid lines are the best fits to the experimental data obtained.

TABLE II. A summary of the experimental results of nonintrinsic a-Si:H films and an intrinsic a-Si:H in the stabilized light soaked state, where N_{DOS} $(\mathrm{cm}^{-3})=\alpha(1.2\ \mathrm{eV})\times 3\times 10^{16}\ \mathrm{cm}^{-3}$.

	Stabilized light soaked state			
a-Si:H films	280 °C	240 °C	200 °C	Intrinsic
σ_D (S/cm)	1.5×10^{-11}	4.2×10^{-12}	4.6×10^{-12}	2.0×10^{-12}
$\mu\tau$ (cm^2/V) ($G=10^{16}$)	1.1×10^{-7}	6.0×10^{-8}	2.0×10^{-8}	1.8×10^{-7}
γ	0.84	0.86	0.85	0.84
α(1.2) (low G) (cm^{-1})	5.5	5.0	5.9	3.70
E_{ov} (meV)	48	48	51	49
$\Delta\alpha$(1.0 eV) (cm^{-1})	1.12	1.10	0.95	0.80
$\alpha(1.2)_{\mathrm{soaked}}/\alpha(1.2)_{\mathrm{ann}}$	4.3	10	21	22
$\mu\tau_{\mathrm{ann}}/\mu\tau_{\mathrm{soaked}}$ ($G=10^{16}$)	350	98	218	11
N_{DOS} (cm^{-3})	1.60×10^{17}	1.50×10^{17}	1.8×10^{17}	1.11×10^{17}
N_{D^0} (cm^{-3}) (ESR)	1.50×10^{17}	1.56×10^{17}	⋯	1.0×10^{17}

dence of α_{ph} on generation rate γ changed to a value around 0.84 in the stabilized soaked state. It decreases if γ is close to unity, generally observed in intrinsic films, and increases to 0.84 if it is less than 0.84 in the annealed state. This is a common characteristic of all a-Si:H films studied whether they are intrinsic or nonintrinsic in the annealed state. The σ_{ph} or the electron $\mu\tau$ products measured at $G=10^{16}$ $\mathrm{cm}^{-3}\,\mathrm{s}^{-1}$ decreased by factors of 218, 98, and 350 for 200, 240, and 280 °C films, respectively. Correspondingly, the α(1.2 eV) measured with low-intensity DBP increased to 5.9 for 200 °C, 5.0 for 240 °C, and 5.5 cm^{-1} for 280 °C film, which are higher than those of intrinsic films. This is consistent with the lower values of stabilized state electron $\mu\tau$ products observed in nonintrinsic a-Si:H films. Net increase in α(1.2 eV), $\alpha(1.2\ \mathrm{eV})_{\mathrm{soaked}}/\alpha(1.2\ \mathrm{eV})_{\mathrm{annealed}}$, is a factor of 21 for 200 °C, 10 for 240 °C, and 4.2 for 280 °C films. This indicates that there is no one-to-one direct correlation between the degradation of photoconductivity and increase of subband-gap absorption, which has been a generally accepted method to study the light induced degradation in the literature.[4,5] Even though there is a distinct increase in $\alpha(h\nu)$ in subband-gap region (between 0.8 and 1.5 eV), the characteristic energy of the valence band tails E_{ov} did not show any significant change after light soaking.

In addition to the increase in α(1.2 eV), there is also an increase in the dependence of $\alpha(h\nu)$ on generation rate in the stabilized soaked state. It is reflected in the values of $\Delta\alpha$ (at 1.0 eV), where it increased to the value close to 1.0 cm^{-1} for all nonintrinsic films even though it showed large variations in the annealed state. This was also observed in intrinsic films. Since $\alpha(h\nu)$ measured with higher-intensity DBP is due to the transitions from the electron occupied states below as well as above midgap, it is an indication that the densities of midgap states below and above the Fermi level increased after light soaking.

Although, the shape of $\alpha(h\nu)$ measured with low generation rate DBP remains unchanged after light soaking, there is a significant change in the shape of $\alpha(h\nu)$ measured with high generation rate DBP. As seen in Fig. 4, the change in the shape of $\alpha(h\nu)$ was clearly observed for the 280 °C film which had a higher density of charged defect states and the R ratio in the annealed state. The change in the shape of $\alpha(h\nu)$ is obvious evidence that there is a distinct difference between the energy distributions of native and light induced midgap states in nonintrinsic a-Si:H films. This behavior was not distinguishable in intrinsic films.

Using the values of α(1.2 eV) measured with low generation rate DBP, the densities of states (DOS) below midgap can be calculated using the $\alpha(1.2\ \mathrm{eV})\times 3\times 10^{16}$ relation.[12] The values calculated from this relation are also summarized in Table II for the nonintrinsic films in the stabilized soaked state. N_{DOS} is found to be 1.8×10^{17} cm^{-3} for 200 °C, 1.5×10^{17} cm^{-3} for 240 °C, and 1.6×10^{17} cm^{-3} for 280 °C films. The density of neutral Si dangling bonds, the D^0, was also directly measured by ESR in the stabilized soaked state for 240 and 280 °C film. The net ESR spin density (after subtracting the density of surface states measured in the annealed state) is 1.56×10^{17} cm^{-3} for 240 °C and 1.5×10^{17} cm^{-3} for 280 °C film, which agrees quite well with the DOS obtained from the $\alpha(1.2\ \mathrm{eV})\times 3\times 10^{16}$ relation.[12] This good agreement was also observed for intrinsic a-Si:H film in the stabilized soaked state. Therefore, the $\alpha(h\nu)$ measured with CPM or low generation rate DBP can be used to estimate the density of neutral Si dangling bonds in the stabilized soaked state for both intrinsic and nonintrinsic a-Si:H films. However, the defect states other than the neutral Si dangling bonds, the D^0, which cause a large degradation of the electron $\mu\tau$ products have to be identified to understand the Staebler–Wronski effect[25] in these nonintrinsic a-Si:H films.

In the analysis of the stabilized light soaked state data, the band-edge and gap states parameters, free carrier capture cross sections, free carrier mobilities, and recombination gap were maintained to be the same as those used in the analysis of the annealed state results. Because of a large decreases in the dark conductivity, a shift in the Fermi level position toward midgap was taken into account. In the modeling of the results of three nonintrinsic films, a downward shift of 70 meV for 280 °C, 20 meV for 240 °C and 10 meV for 200 °C film were made. The charge neutrality in the dark is mainly determined by the densities of the D^+ and the D^- states.

The best fits to the results of σ_{ph} and $\alpha(h\nu)$ in the stabilized soaked state are shown as solid lines in Figs. 3 and 4 for nonintrinsic a-Si:H films at 200 and 280 °C, respectively. The parameters derived for the annealed and stabilized soaked states are also summarized in Table III. For these nonintrinsic films, the densities of both the neutral and charged defect states increase, however, neutral defect states D^0 increase faster. The densities of the D^0 states N_{D^0} are slightly higher than those in intrinsic films. The R ratio decreases drastically from its annealed state value, where it becomes similar to that in the intrinsic films. It ranges between 1.5 and 1.8, as compared to the values having a range from 2.25 to 15 in the annealed state. These values of R ratio give rise to similar dependence of $\alpha(h\nu)$ on generation rate, which is around 1.0 cm^{-1} for both the intrinsic and nonin-

TABLE III. Parameters obtained from the numerical analysis of steady-state photoconductivity and subband-gap absorption data for the native and light induced neutral and charged defect states in the band gap of nonintrinsic (undoped) *a*-Si:H films and those of an intrinsic *a*-Si:H in the annealed and stabilized light soaked states, where: N_{DOS} (cm^{-3})$=\alpha(1.2\ \mathrm{eV})\times 3\times 10^{16}$ cm^{-3}; L_{Dp} (SSPG) was measured using the SSPG technique at generation rate close to 2×10^{20} $\mathrm{cm}^{-3}\,\mathrm{s}^{-1}$; L_{Dp} (calculated)$=(2\mu_p\tau_p kT/e)^{0.5}$, where $\mu_p\tau_p$ was calculated at $G=2\times 10^{20}$ $\mathrm{cm}^{-3}\,\mathrm{s}^{-1}$ from the numerical analysis using the best fit parameters; N_D (cm^{-3}) (ESR) was directly measured by the ESR technique. NM: not measured.

a-Si:H films	280 °C		240 °C		200 °C		Intrinsic	
Parameters/State	Annealed	Soaked	Annealed	Soaked	Annealed	Soaked	Annealed	Soaked
E_{ov} (meV)	48	48	48	48	49	51	49	49
E_{oc} (meV)	21	40	21	39	21	40	21	35
N_{D^0} (cm^{-3})	8×10^{15}	1.40×10^{17}	8×10^{15}	1.60×10^{17}	8×10^{15}	2.0×10^{17}	4.50×10^{15}	1.0×10^{17}
E_{D^0} (eV) (from VB)	0.78	0.78	0.79	0.79	0.80	0.80	0.78	0.78
N_{D^+} (cm^{-3})	6.0×10^{16}	1.10×10^{17}	1.60×10^{16}	1.40×10^{17}	9.0×10^{15}	1.8×10^{17}	3.0×10^{15}	6.0×10^{16}
E_{D^+} (eV) (from VB)	1.36	1.22	1.30	1.26	1.36	1.22	1.28	1.28
N_{D^-} (cm^{-3})	6.0×10^{16}	1.10×10^{17}	1.60×10^{16}	1.40×10^{17}	9.0×10^{15}	1.8×10^{17}	3.0×10^{15}	6.0×10^{17}
E_{D^-} (eV) (from VB)	0.56	0.48	0.57	0.48	0.56	0.48	0.50	0.50
N_{D^0} (cm^{-3}) (ESR)	NM	1.50×10^{17}	NM	1.56×10^{17}	NM	⋯	NM	1.08×10^{17}
N_{DOS} (cm^{-3})	3.6×10^{16}	1.60×10^{17}	1.60×10^{16}	1.50×10^{17}	8.4×10^{15}	1.8×10^{17}	4.8×10^{15}	1.1×10^{17}
$R=(N_{D^-}+N_{D^+})/N_{D^0}$	15	1.5	4.0	1.7	2.25	1.8	1.4	1.2
L_{Dp} (Å) (SSPG)	1.18×10^{3}	8.80×10^{2}	1.22×10^{3}	7.90×10^{2}	1.02×10^{3}	5.90×10^{2}	⋯	⋯
L_{Dp} (Å) (calculated)	1.09×10^{3}	9.10×10^{2}	1.19×10^{3}	8.0×10^{2}	1.14×10^{3}	7.40×10^{2}	1.02×10^{3}	8.50×10^{2}

trinsic films. However, in the nonintrinsic films, in order to maintain the charge neutrality in the dark and self-consistently fit the very large degradation in the photoconductivities and subband-gap absorption, it was necessary to have the charged defect states in the stabilized state to be closer to the valence-band edge. The D^- states are at about 0.5 eV, and the D^+ states are 1.22–1.26 eV from the valence-band edge similar to those in the intrinsic films. As in the case of intrinsic films, it was also necessary to increase the characteristic energy parameter of the conduction band tails E_{oc} in the stabilized soaked state in order to fit the γ and σ_{ph} data at the highest generation rates.[12]

The densities of the neutral defect states N_{D^0} obtained from the $\alpha(1.2\ \mathrm{eV})\times 3\times 10^{16}$ relation are also shown in Table III. Although this relation cannot be used to estimate the density of the neutral defect states in nonintrinsic films in the annealed state, as discussed in the previous subsection, N_{D^0} values obtained from this relation for the stabilized light soaked states are within less than 15% of the D^0 densities derived from the best fits. Furthermore, the net densities of ESR spins in the stabilized soaked state (after subtracting the contribution of surface/interface defect states) were measured as 1.56×10^{17} cm^{-3} for 240 °C and 1.5×10^{17} cm^{-3} for 280 °C film; which agree very well with the values of 1.6×10^{17} and 1.4×10^{17} cm^{-3} derived from the numerical analysis, respectively.

In addition to the detailed analysis of the σ_{ph} and $\alpha(h\nu)$ which are determined by electrons, measurements of the hole diffusion lengths L_{Dp} were also carried out on these nonintrinsic films in the stabilized soaked state. From the best fit parameters, the $\mu\tau$ values for holes at a generation rate of 2×10^{20} $\mathrm{cm}^{-3}\,\mathrm{s}^{-1}$ were used to calculate $L_{Dp}=(2\mu_p\tau_p kT/e)^{1/2}$,[24] assuming the same hole mobility, $\mu_p=0.2$ $\mathrm{cm}^2/\mathrm{V\,s}$, as in the annealed state. A very good agreement was found between the experimental results and those calculated from the hole $\mu\tau$ products. These results also listed in Table III. The additional results on the hole diffusion lenghts and those of ESR measurements indicate that midgap state parameters derived here are reliable and that both the charged and neutral defect states are created by light.

C. Kinetics of Staebler–Wronski effect

It was shown that both neutral and charged defect states are created during the light soaking. Since the films studied here have different R ratios in the annealed state and since they exhibit similar characteristics at the stabilized soaked state, it is important to study the kinetics of light induced defect creation and their effects on $\alpha(h\nu)$ and σ_{ph}. The effect of light intensity on degradation was investigated on an intrinsic film whose characteristics are given in Tables I and II. The results of $\alpha(1.2\ \mathrm{eV})$ measured with low generation rate DBP are shown in Fig. 5(a) as a function of time for three different illumination intensities, the first of which was obtained using 100 $\mathrm{mW/cm}^2$ white light from an ELH tungsten–halogen lamp, and the second one was under 1 $\mathrm{W/cm}^2$ white light (approximately 10 suns) from ELH tungsten-halogen lamp, and the last one was under $1\mathrm{W/cm}^2$ ELH white light illumination after which a red filter was inserted to cut out $\lambda<610$ nm, which would ensure uniform absorption of illumination. In Fig. 5(b) the corresponding changes in σ_{ph} are shown for the above illuminations. Light soaking with 100 $\mathrm{mW/cm}^2$ white light was made through the film up to 1000 h and was continued through the opposite side for an additional 700 h. Steady states (stabilized soaked state) of photoconductivity and $\alpha(1.2\ \mathrm{eV})$ were obtained after 1000 h. The changes in $\alpha(1.2\ \mathrm{eV})$ increased according to $t^{0.24}$ and the σ_{ph} degradation followed $t^{-0.26}$ dependence. To see the effect of uniform light soaking, a red filter (RG-610) after 10 suns of white light were used for accelerated degradation. In this case, the stabilized soaked state was obtained after 300 h with soaking through one side of sample only. Both $\alpha(1.2\ \mathrm{eV})$ and σ_{ph} reached different stabilized state values from that of 100 $\mathrm{mW/cm}^2$ white light soaking and followed almost the same dependencies on time. Further ac-

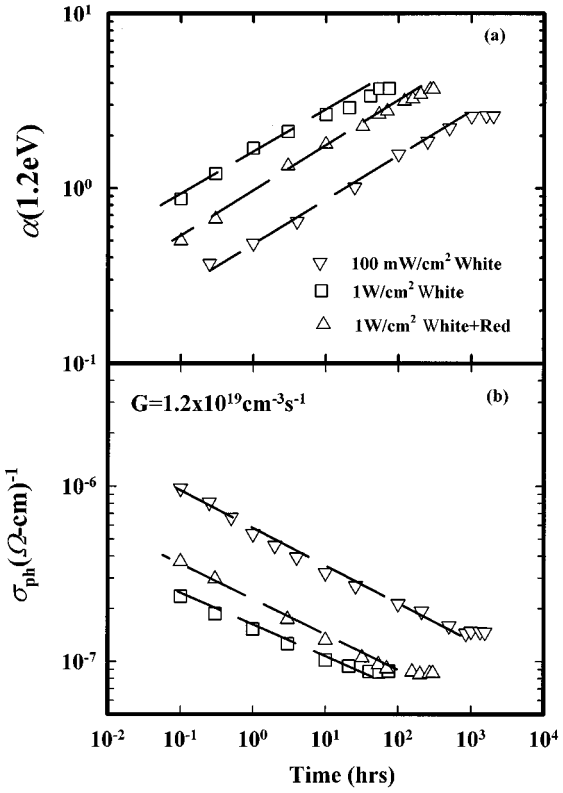

FIG. 5. (a) The changes in $\alpha(1.2\ \text{eV})$ measured with low generation rate DBP, and (b) the changes in σ_{ph} measured at $G=1.2\times10^{19}\ \text{cm}^{-3}\,\text{s}^{-1}$, as a function of soaking time for the intensities of 100 mW/cm^2 white light, 1 W/cm^2 white light, and 1 W/cm^2 white light+red filter ($\lambda>610$ nm) for an intrinsic a-Si:H thin film.

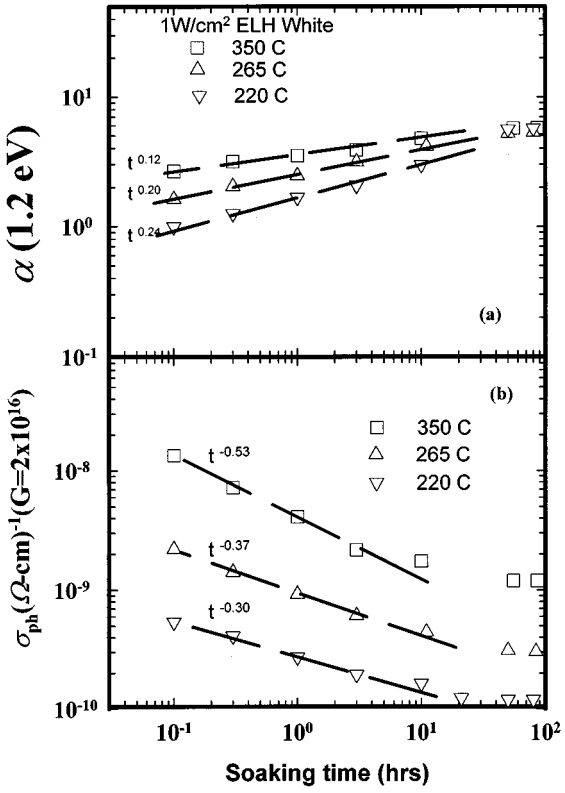

FIG. 6. (a) The changes in $\alpha(1.2\ \text{eV})$ measured with low generation rate DBP, and (b) the changes in σ_{ph} measured at $G=2\times10^{16}\ \text{cm}^{-3}\,\text{s}^{-1}$, as a function of soaking time. The undoped (nonintrinsic) a-Si:H thin films were degraded with the intensity of 1 W/cm^2 ELH white light intensity.

celerated light soaking was carried out with a higher intensity (10 suns) of ELH white light source. The light soaking was carried out through one side of the sample. Even though the steady state was reached after 60 h of soaking (even sooner than red light soaking), the values of $\alpha(1.2\ \text{eV})$ and σ_{ph} were the same as red light soaking having the same time dependencies. Furthermore, high-intensity ELH white light degradation was also studied on other intrinsic a-Si:H films.[18] They all exhibited similar degradation kinetics for σ_{ph} and $\alpha(1.2\ \text{eV})$ with the similar time dependencies given above.

In addition to the above experiments, we investigated the accelerated degradation using a high-intensity xenon white light source of 3 W/cm^2 (data not shown). It was found that it was not possible to reach the stabilized soaked state with illumination through one side of the sample. Subsequent illumination through the opposite side of the sample decreased σ_{ph} more and correspondingly increased $\alpha(1.2\ \text{eV})$. The stabilized state values of $\alpha(1.2\ \text{eV})$ and σ_{ph} were the same as those for high-intensity white and red light soakings. Because of the nonuniform generation of defects with xenon light source, care has to be taken when studying degradation with xenon white light source on both films and solar cell structures.

The rates of light induced degradation on several nonintrinsic (undoped) a-Si:H films were investigated using 1 W/cm^2 white light illumination only. These films prepared under the same conditions as those studied here were deposited at substrate temperatures between 220 and 350 °C. Their annealed and stabilized state characteristics are similar to those of nonintrinsic films discussed above. The results of $\alpha(1.2\ \text{eV})$ measured using low-intensity DBP and the corresponding changes in σ_{ph} measured at $G=2\times10^{16}\ \text{cm}^{-3}\,\text{s}^{-1}$ are shown in Figs. 6(a) and 6(b) as a function of soaking time, respectively. The $\alpha(1.2\ \text{eV})$ follows different time dependencies for different films and varies from $t^{0.12}$ to $t^{0.24}$. The film deposited at 220 °C exhibits almost the same time dependence as intrinsic films. Then, as T_s increased, the time dependence of $\alpha(1.2\ \text{eV})$ decreased. However, corresponding photoconductivity changes in Fig. 6(b) show much faster degradation for higher T_s film and slower degradation for low T_s films. These results clearly show that there is no unique rate for defect creation in a-Si:H films as implied by the bond breaking model.[4]

According to this model, the σ_{ph} is inversely proportional to $\alpha(h\nu)$ or to the density of midgap states N_{DOS} [$\sigma_{ph}\propto1/\alpha(h\nu)$ or $1/N_{DOS}$]. The σ_{ph} measured at low generation rates can be correlated with the subband-gap absorption measured by CPM or low generation rate DBP because at lower generation rates the splitting of quasi-Fermi levels is small and only the small fraction of midgap states above the Fermi level is involved in the recombination kinetics. Using the results in Figs. 6(a) and 6(b) we replotted the changes in σ_{ph} measured at low generation rates versus corresponding changes in $1/\alpha(1.2\ \text{eV})$. This is shown in Fig. 7 including the

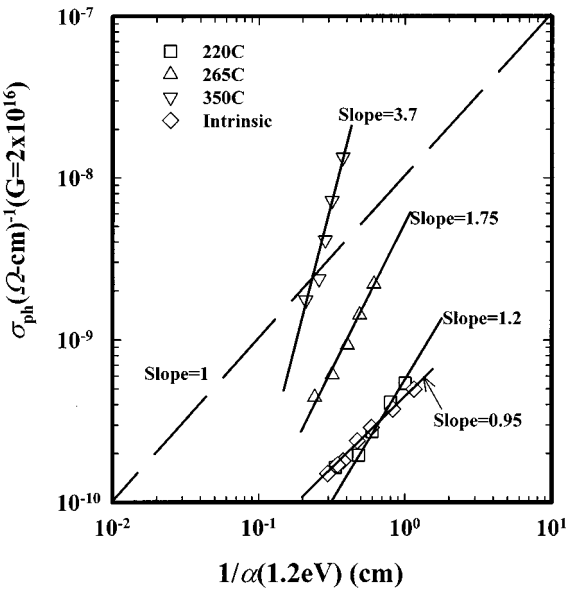

FIG. 7. (a) The changes in $1/\alpha(1.2\ \text{eV})$ measured with low generation rate DBP vs the changes in σ_{ph} measured at $G=2\times10^{16}\ \text{cm}^{-3}\ \text{s}^{-1}$, degraded with the intensity of 1 W/cm^2 ELH white light, for an intrinsic and different nonintrinsic (undoped) a-Si:H thin films.

results of the intrinsic film studied above. These results show that the changes in σ_{ph} is not directly proportional to the changes in $1/\alpha(1.2\ \text{eV})$. The slope changes from 0.95 to 3.7 indicating that in nonintrinsic films $\alpha(1.2\ \text{eV})$ measured by CPM or low generation rate DBP is dominated not only by the neutral Si dangling bonds, the D^0, but also the charged defect states, the D^+ and D^-.[1,29]

Using the above results it can be concluded that red light and ELH white light illumination provide uniform creation of defects on films with thicknesses of around 1 μm. The kinetics of light induced degradation is similar for intrinsic films. It was obtained from the analysis that the R ratios are low for these films in the annealed state and did not show a drastic decrease in the stabilized soaked state. This means that both the neutral and charged defect states are created with almost the same rate in intrinsic films. However, nonintrinsic films exhibit wide range of degradation kinetics with different time dependencies. This is because of the differences both in the densities of the neutral and charged defect states and in the R ratios for the annealed state. The R ratio decreases for all films in the stabilized soaked state to a value between 1.5 and 1.8, and this implies that during the light soaking the neutral and charged defect states are created with different rates for different sample.

IV. DISCUSSION

It was shown here that the distribution of the charged defect states can be used for self-consistent analysis of the results of the steady-state photoconductivity and subband-gap absorption for a wide range of generation rates in nonintrinsic a-Si:H films both in the annealed and stabilized soaked states. The differences in the ratios of the charged to neutral defect density and the densities of the charged defect states in the different materials can explain different results in the annealed and light soaked states.

In the annealed state, the R ratio in nonintrinsic (undoped) films changes from 2.25 to 15, which is much higher than the values obtained for intrinsic a-Si:H films.[13] The higher values of the R ratio obtained on these films are consistent with the results obtained from the LESR[6–11] and electron spin echo-envelope modulation (ESEEM)[30,31] experiments. When the R ratio increases, there is larger contribution to the subband-gap absorption from the charged defect states which results in higher $\alpha(h\nu)$, even at low generation rates, as well as higher $\Delta\alpha(1.0\ \text{eV})$. In intrinsic films, $\Delta\alpha(1.0\ \text{eV})$ is low, which changes from 0.06 to 0.1 cm^{-1}; however, it is much higher in the nonintrinsic films where in the annealed state $\Delta\alpha(1.0\ \text{eV})$ increases from 0.1 to 0.90 cm^{-1}. In the case of higher R values, the $\alpha(h\nu)$ measured with low generation rate DBP or using CPM is dominated by the neutral and charged defect states. Therefore, $\alpha(1.2\ \text{eV})$ can no longer be directly related to the densities of the neutral defect states located below the Fermi level. As seen from Table III, in the intrinsic films, the densities of the D^0 states derived from the analysis were very close to those obtained from the $\alpha(1.2\ \text{eV})\times3\times10^{16}$ relation. On the other hand, this relation overestimates the densities of neutral defect states in nonintrinsic films.

Furthermore, the higher R ratios have a drastic effect on the free electron lifetimes obtained from the steady-state photoconductivity measurements. Because the negatively charged acceptor-like states below the Fermi level have a very small capture cross sections for electrons, they act as sensitizing states as proposed by Rose.[32] Under light illumination, they are the only recombination centers that are empty because the donor-like states above the E_F are mostly filled with electrons due to their higher capture cross sections. This results in higher electron lifetimes and photoconductivity. As R increases so does the sensitization and, hence, photoconductivity. This is the only physical reason to explain the higher photoconductivities measured on defective undoped a-Si:H films.

Because of the large differences in the densities of charged defects, intrinsic and nonintrinsic films exhibit completely different degradation kinetics. Photoconductivities degrade according to a time dependence given by t^{-x}, where x is 0.26 for intrinsic films and changes from 0.30 to 0.53 in nonintrinsic films studied here. Correspondingly, $\alpha(1.2\ \text{eV})$ increases according to time dependence t^y, where y is 0.24 for intrinsic films and changes from 0.24 to 0.12 in nonintrinsic films. The results here clearly show that there is no unique relation for the kinetics of the Staebler–Wronski effect in a-Si:H films such as the $t^{1/3}$ rule ($\sigma_{ph}\propto Gt^{1/3}$ or $N_{DOS}\propto Gt^{1/3}$, where G is constant generation rate), which was based on two Gaussian distributions of the D^-,D^0 states with positive correlation energy.[4] Therefore, there is no direct correlation between the degradation of σ_{ph} and the corresponding increase of subband-gap absorption.

In the stabilized soaked state, the R ratio decreased drastically for all nonintrinsic a-Si:H films and very slightly for intrinsic films. It reached to values close to 1.0. The density

of the neutral defect states created is higher than those of the positively and negatively charged defect states. Thus, the subband-gap absorption measured at low generation rate DBP or using CPM is mainly dominated by the density of the neutral defect states. In contrast with the case in the annealed state, there are good agreements between the densities of neutral defects derived and those obtained from $\alpha(1.2\ \text{eV})\times 3\times 10^{16}$ relation. Furthermore, density of the neutral defect states obtained from the analysis are very close to those directly measured by ESR for both intrinsic and nonintrinsic a-Si:H films.

In addition to the results discussed above, which depend on the majority carrier properties, we have also measured minority carrier, hole, diffusion lengths using the SSPG technique on the same nonintrinsic a-Si:H films in the same annealed and stabilized soaked states. Excellent agreement was found between the experimental diffusion lengths and those derived from the best fit results of numerical analysis. Therefore, using SSPG technique and the results of numerical analysis of photoconductivity and subband-gap absorption on thin films, important information about the minority carrier hole mobility can be obtained. This will be an extremely important parameter for the modeling of solar cell device characteristics where both minority and majority carriers play a role.

Since the R ratio is different for different films in the annealed state and decreases to almost the same value in the stabilized soaked state, this brings about different rates for the creation of neutral defects and charged defects for different films so that steady-state photoconductivity and subband-gap absorption follow different time dependencies for different films. This is clearly seen in Fig. 6 for the measurements carried out in different nonintrinsic a-Si:H films; however, intrinsic films showed almost the same degradation kinetics since they all had similar R ratios in the annealed state. In the case of nonintrinsic films, the $\alpha(h\nu)$ measured with low generation rate DBP or CPM during the intermediate light soaking periods will still be under the influence of both the neutral and the charged defect states. Therefore, it will be inappropriate to characterize the kinetics of light induced defect creation using the ''the stretched exponentials model'' or so-called ''impurity model''[5] since this model assumes only the neutral defect states as the main defect created during the light soaking and characterizes them using CPM spectrum.

It is also interesting to note that an increase in the characteristic energy of the conduction band tail states was inferred from the modeling of the stabilized state in both intrinsic and nonintrinsic a-Si:H films even though no significant change was detected for E_{ov}. At this time the reason for this phenomenon is not known although the similar changes have been reported by Takada and Fritzche[33] based on their results of drift mobilities. They explained the decrease in drift mobility upon the light degradation of n-type a-Si:H films by an increase in the density of the conduction-band-tail states within 0.35 eV below the electron mobility edge or by decrease of microscopic mobility. More recently, Han *et al.* have studied the transient photocharge measurements on annealed and light soaked undoped a-Si:H films.[34] They found that the coalescence of transients in early time regime is less perfect in the light soaked state due to an increase in recombination rate. Then they speculated that there is a light induced change in the conduction band tail regime.

The evidences for the charged defect states in the bulk of a-Si:H films and their effects on different measurements was extensively discussed by Branz and Silver[29] and later by Powell and Dean;[35] however, for the significance of the results derived here, we revisit some of those experimental results in the literature. As mentioned earlier, the first LESR results on a-Si:H indicated roughly equal electron and hole absorption lines and it was a conclusion that an insignificant fraction of dangling bonds is charged in undoped a-Si:H.[2] Later, Ristein and co-workers[7] and Hautala and co-workers[9] carried out a more careful study of ESR and LESR using band-gap and below band-gap light on thick (8 and 15 μm) a-Si:H films. They found that LESR with band-gap light gives equal electron-to-hole absorption lines; however, LESR with IR light increased the ratio of the narrow line (electron line) to the broad absorption line (hole line). This disproportionality was attributed to excitations of electrons from the D^- states located close to the valence-band edge to the conduction-band-tail states. They concluded that the densities of the D^- states were higher than the density of the D^0 states measured with ESR in the dark. Unfortunately, they were able to explain these results using the two Gaussian distributions of bulk defect states, and since that was not possible, they attributed the observed phenomena to the high densities of surface/interface states even in 15-μm-thick films. In addition, similar LESR results were reported by Shimizu *et al.* that a large fraction of defects states in undoped a-Si:H is charged defect states.[6] They speculated that these charged defect states are due to nitrogen impurities in a-Si:H films. Later, these results were reinterpreted by Branz[36] as the bulk charged defect-states in a-Si:H. More recently, detailed comparisons of absorption data and spin density using LESR experiments have shown that there are systematic deviations from the proportionality between electron and hole absorption lines.[11] It was found that LESR measurements carried out at high intensities result in proportional electron and hole absorption lines. However, low-intensity LESR experiment shows a disproportionality, where the hole spin density is much higher than total electron density. The explanation of the low-intensity LESR results required the presence of a broad band of positively charged defects, the D^+, in the region of 0.4 0.70 eV below the conduction-band edge. To maintain the charge neutrality in the dark, these positively charged states must be balanced by negatively charged states below the Fermi level. Such D^- states were also detected in an IR-LESR experiment by Ristein and co-workers.[7,9] In addition, Schumm and co-workers also quantified the ratio of charged to neutral defect density, R, both in the annealed and light soaked states. They reported that the values of R ratio change from 5 to 10 in the annealed films which then decreased to around 1.0 in the light soaked state. These fundamental evidences on the charged defect states in the gap of undoped a-Si:H films are

consistent with our results derived from the analysis of photoconductivity and subband-gap absorption.

The supporting experimental results just discussed and the self-consistent analysis of the photoconductivities and subband-gap absorption spectra over a wide range of generation rates in various *a*-Si:H films are strong evidences for the distribution of neutral and charged defects in *a*-Si:H materials. The positively charged defect states D^+ are located above the Fermi level and the neutral D^0 and the negatively charged D^- states are located below the Fermi level. Models proposed for undoped *a*-Si:H materials must include such states both in the annealed and light soaked states. Therefore models that do not result in charged Si dangling bonds such as the bond breaking model[4] and the impurity model[5] appear to be inadequate for explaining the Staebler–Wronski effect in *a*-Si:H films.

The first model that considered the charged defect states was proposed by Adler,[1] with significant densities of charged Si dangling bonds having negative correlation energy already present in the annealed state. Although this model can explain the native charged defect states in *a*-Si:H films, it is not sufficient for explaining the light induced degradation. According to this model, photogenerated electrons and holes are trapped in the previously present charged Si dangling bonds which are then converted to the neutral Si dangling bonds. This leads to an increase in the densities of the D^0 and to a decrease of charged dangling bonds. Both our and LESR results indicate that both the charged and neutral defects are created by light. Therefore, the original Adler model is inadequate to explain the Staebler–Wronski effect in *a*-Si:H films.

The potential fluctuations model proposed by Branz and Silver[29] uses a defect pool model in which there is no weak Si–Si bond breaking mechanism involved. They proposed that large densities of charged dangling bonds are present in the annealed state due to potential fluctuations. In this model, the D^+ states are above and the D^- states are below the Fermi level. Similar to Adler's model, during the light soaking photogenerated electrons and holes are trapped in the charged states which are then converted to the D^0 states. Consequently the densities of the D^0 states increase and those of charged defect states decrease after light soaking, which is in disagreement with our findings as well as that of LESR experiments.

The defect pool model used by Schumm and Bauer[37] involves a hydrogen entropy contribution to the chemical potential of defects and a weak Si—Si bond conversion process. Simultaneous formation of defects in all three charge states are considered with different microscopic reactions involving zero, one, and two Si—H bonds mediating a weak Si—Si bond breaking process. The derived densities and energy location of the charged and neutral defect states have more charged than neutral defect states in the annealed films. Recently, Powell and Dean[35] considered a defect pool model, ''the improved defect pool model,'' with wide pool and two Si—H bonds mediating the weak Si—Si bond breaking reaction. The energy spectra and the densities of charged and neutral defect states were calculated using inputs from their experiments on thin-film transistors and a ratio of charged to neutral defect density of 4 was obtained for material with $E_F=0.85$ eV from the conduction-band edge. The energy positions for charged and neutral defect states they derived are very close to those obtained from our analysis, especially the total densities of states ($D^+ + D^- + D^0$) obtained for the film deposited at $T_s=240$ °C with a similar Fermi level position is the same as their results. Although this model was used to predict the nature, densities, and energy spectra of many observations in the annealed state, no results on light soaked materials have been reported. However, recently Schumm and co-workers[11] explained their LESR and subband-gap absorption results using their defect pool model. They found that during light soaking the densities of both neutral and charged defect states increase with the D^0 states increasing more quickly. The *R* ratio decreases from about 5 to 10 in the annealed state to around 1.0 in the light soaked state.

V. CONCLUSIONS

It was found that only the distribution of the charged defect states can be successfully applied to the detailed analysis of the steady-state photoconductivity and subband-gap absorption results of nonintrinsic (undoped) *a*-Si:H thin films over a wide range of generation rates both in the annealed and stabilized light soaked states. This distribution includes exponential valence and conduction band tail states, a band of positively charged defect states located above the Fermi level, and two bands of the neutral and negatively charged defect states located below the Fermi level.

In the annealed state, the energy location of the neutral defect states is around 0.80 eV from the valence band mobility edge, which is similar to those obtained in intrinsic *a*-Si:H films; however, charged defect states are located at slightly higher energies in nonintrinsic *a*-Si:H films. Even though the densities of the neutral defect states do not change significantly, those of positively and negatively charged defect states and the *R* ratio are drastically different for different films. These results derived for the densities and the *R* ratio are consistent with those determined from the ESR and LESR measurements.[11] Because of the higher densities of the charged defect states dominating in the annealed state, the subband-gap absorption spectrum measured by CPM or low generation rate DBP can no longer be correlated directly with the densities of neutral Si dangling bonds.

In the stabilized light soaked state, almost the same gap state distributions and parameters as in the annealed state have been used in the analysis. It was found that both the neutral and charged defect states are created by light. The *R* ratio decreases drastically to a value close to 1, which is similar to those of intrinsic *a*-Si:H films. Because of that, in each film the neutral and charged defect states are created with different rates so that photoconductivity and subband-gap absorption follow different degradation kinetics. Thus there is no unique degradation kinetics for *a*-Si:H. The densities of the neutral defect states derived from the analysis were directly correlated with those measured by ESR and excellent agreement was obtained. In addition to these results, minority carrier hole diffusion lengths measured by the SSPG technique on the same films were correlated with

those calculated using the hole $\mu\tau$ products derived from the best fits of modeling. Very good agreements were obtained for different films both in the annealed and stabilized light soaked states. This suggests that the SSPG technique and detailed numerical analysis of photoconductivity and subband-gap absorption spectra can be used to obtain more accurate information about the value of free hole mobility μ_p, which is extremely important for the modeling of solar cells and other a-Si:H based devices.

In conclusion, the results obtained in this study indicate that the charged defect states are much better representations of the native and light induced bulk defect states in undoped hydrogenated amorphous silicon thin films. Care must be taken for the characterizations of these defects in different a-Si:H films using the subband-gap absorption and other methods and their effects on the operations of solar cell devices must be taken into account.

ACKNOWLEDGMENTS

Most of this study was carried out at Electronic Materials Processing and Research Laboratory, The Pennsylvania State University. This work was supported by Electric Power Research Institute (EPRI) Thin Film Solar Cell Program and New Energy Development Organization (NEDO) International Joint Research Grant. The authors want to thank Drs. R. Collins, Youming Li, C. M. Fortmann, and S. Fonash for helpful discussions, Dr. T. J. McMahon for ESR measurements, and Dr. R. Crandall for SSPG measurements. One of us (M.G.) would like to thank the Turkish Government, Ministry of National Education, for a partial Ph.D. scholarship during his stay in the U.S.A.

[1] D. Adler, Sol. Cells **9**, 113 (1983).
[2] R. A. Street and D. K. Biegelsen, Solid State Commun. **33**, 1159 (1980).
[3] W. B. Jackson and N. M. Amer, Phys. Rev. B **25**, 5559 (1982).
[4] M. Stutzmann, W. B. Jackson, and C. C. Tsai, Phys. Rev. B **32**, 23 (1985).
[5] D. Redfield and R. H. Bube, Appl. Phys. Lett. **54**, 1037 (1989); in *Amorphous Silicon Materials and Solar Cells*, AIP Conf. Proc., Vol. 234 (AIP, New York, 1991), p. 66.
[6] T. Shimizu, H. Kidoh, X. Xu, A. Morimoto, and M. Kumeda, Mater. Res. Soc. Symp. Proc. **118**, 665 (1988).
[7] J. Ristein, J. Hautala, and P. C. Taylor, Phys. Rev. B **40**, 88 (1989).
[8] S. Yamasaki, H. Okushi, A. Matsuda, and K. Tanaka, Phys. Rev. Lett. **65**, 756 (1990).
[9] J. Hautala, P. C. Taylor, and J. Ristein, in *Amorphous Silicon Materials and Solar Cells*, AIP Conf. Proc., Vol. 234 (AIP, New York, 1991), p. 170.
[10] Z. M. Saleh, H. Tarui, S. Tsuda, S. Nakano, and Y. Kuwano, Mater. Res. Soc. Symp. Proc. **258**, 359 (1992).
[11] G. Schumm, W. B. Jackson, and R. A. Street, Phys. Rev. B **48**, 14 198 (1993).
[12] M. Gunes, C. R. Wronski, and T. J. McMahon, J. Appl. Phys. **76**, 2260 (1994).
[13] M. Gunes, R. W. Collins, and C. R. Wronski, Mater. Res. Soc. Symp. Proc. **336**, 413 (1994).
[14] S. Lee, M. Gunes, C. R. Wronski, N. Maley, and M. Bennett, Appl. Phys. Lett. **59**, 1578 (1991).
[15] J. G. Simmons and G. W. Taylor, Phys. Rev. B **4**, 502 (1971).
[16] J. Tauce, in *Optical Properties of Solids*, edited by F. Abeles (North-Holland, New York, 1972), p. 279.
[17] S. Lee, S. Kumar, C. R. Wronski, and N. Maley, J. Non-Cryst. Solids **114**, 316 (1989).
[18] M. Gunes, Ph.D. thesis, The Pennsylvania State University, University Park, PA 16802, 1995.
[19] Z. E. Smith, V. Chu, K. Shephard, S. Aljishi, D. Slobodin, J. Kolodzey, S. Wagner, and T. L. Chu, Appl. Phys. Lett. **50**, 1521 (1987).
[20] Y. Tang and R. Braunstein, Appl. Phys. Lett. **66**, 721 (1995).
[21] M. Gunes, Y. M. Li, R. M. Dawson, C. M. Fortmann, and C. R. Wronski, in *Proceedings of IEEE XIII Photovoltaic Specialists Conference* (IEEE, New York, 1993), p. 885.
[22] M. Gunes and C. R. Wronski, Appl. Phys. Lett. **61**, 678 (1992).
[23] C. E. Nebel, R. A. Street, N. M. Johnson, and J. Walker, Mater. Res. Soc. Symp. Proc. **297**, 97 (1993).
[24] I. Balberg, Mater. Res. Soc. Symp. Proc. **258**, 693 (1992), and references therein.
[25] D. L. Staebler and C. R. Wronski, Appl. Phys. Lett. **31**, 292 (1977).
[26] H. Dersch, J. Stuke, and J. Beichler, Appl. Phys. Lett. **38**, 456 (1980).
[27] P. V. Santos, W. B. Jackson, and R. A. Street, in *Amorphous Silicon Materials and Solar Cells*, AIP Conf. Proc., Vol. 234 (AIP, New York, 1991), p. 51.
[28] C. R. Wronski, in *Semiconductors and Semimetals*, edited by J. Pankove (Academic, New York, 1984), Vol. 21, Part C, p. 347.
[29] H. Branz and M. Silver, Phys. Rev. B **42**, 7420 (1990).
[30] J. Isoya, S. Yamasaki, H. Okushi, A. Matsuda, and K. Tanaka, Phys. Rev. B **47**, 7013 (1993).
[31] S. Yamasaki and J. Isoya, J. Non-Cryst. Solids **164–166**, 169 (1993).
[32] A. Rose *Concepts in Photoconductivity and Allied Problems* (Wiley, New York, 1963).
[33] J. Takada and H. Fritzche, Mater. Res. Soc. Symp. Proc. **95**, 571 (1987).
[34] D. Han, D. C. Melcher, E. A. Schiff, M. Silver, Phys. Rev. B **48**, 8658 (1993).
[35] M. J. Powell and S. C. Dean, Phys. Rev. B **48**, 10 815 (1993).
[36] H. M. Branz, Phys. Rev. B **41**, 7887 (1990).
[37] G. Schumm and G. H. Bauer, J. Non-Cryst. Solids **137&138**, 315 (1991).